# Supporting Information

## Increasing Porosity in Hydrogen-bonded Organic Frameworks for Low-$\kappa$ Interlayer Dielectric

*Yanchao Song*[a], *Shiyuan Zhu*[a], *Lizhen Liu*[b], *Shengchang Xiang*[a], *Zizhu Yao**[a], *Zhangjing Zhang**[a]

[a] Fujian Provincial Key Laboratory of Polymer Materials, College of Chemistry and Materials Science, Fujian Normal University, 32 Shangsan Road, Fuzhou 350007, China.

[b] School of Materials Science and Engineering, Fujian University of Technology, Fujian 350118, China.

*Corresponding author. E-mail address: yaozizhu@fjnu.edu.cn (Z. Yao); zzhang@fjnu.edu.cn (Z. Zhang).

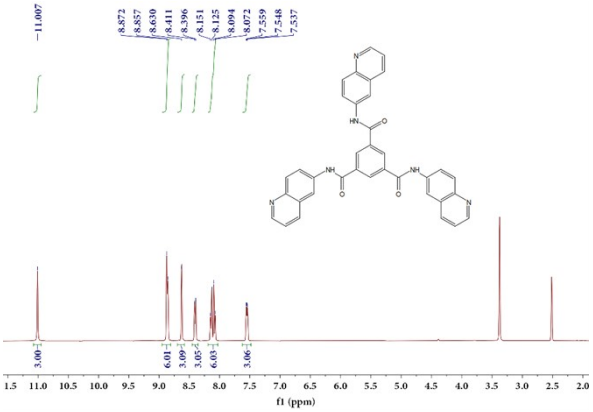


**Fig. S1** $^{1}$H NMR spectrum of $N^{1}$, $N^{3}$, $N^{5}$-tris (quinolin-6-yl) benzene-1,3,5-tricarboxamide.

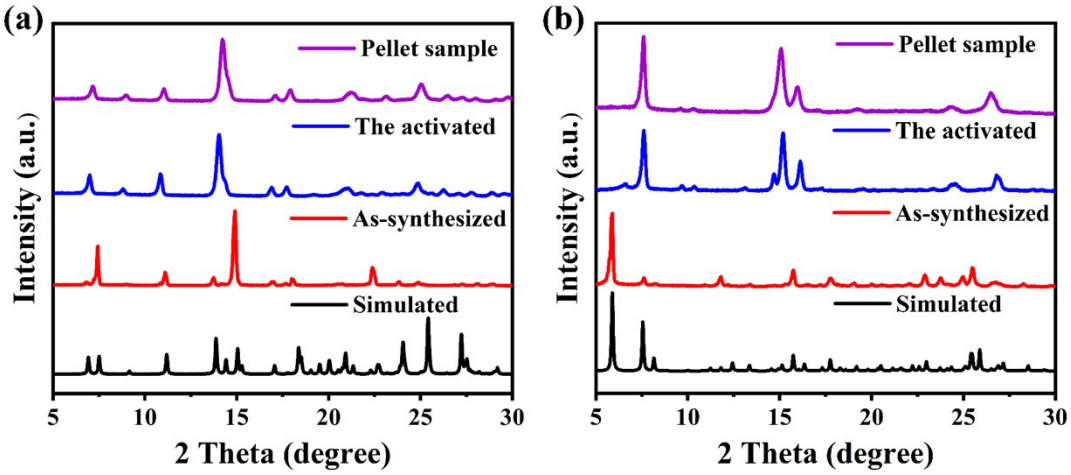


**Fig. S2** The PXRD pattern of (a) **HOF-FJU-56** and (b) **HOF-FJU-57**.

The synthesized **HOF-FJU-56** and **HOF-FJU-57** are characterized by powder X-ray diffraction (PXRD) (Fig. S2) which show all the peak positions of the experimental PXRD patterns measured at room temperature are matching closely with simulated results transformed using single crystal data, thus further conforming the high purity of the synthesized samples. The PXRD of samples after activation (denoted as The activated) and pressing into pellets (denoted as Pellet sample) exhibits that both frameworks retained but with slightly shifted in $2\theta$ values, indicating the flexible nature of the two frameworks.

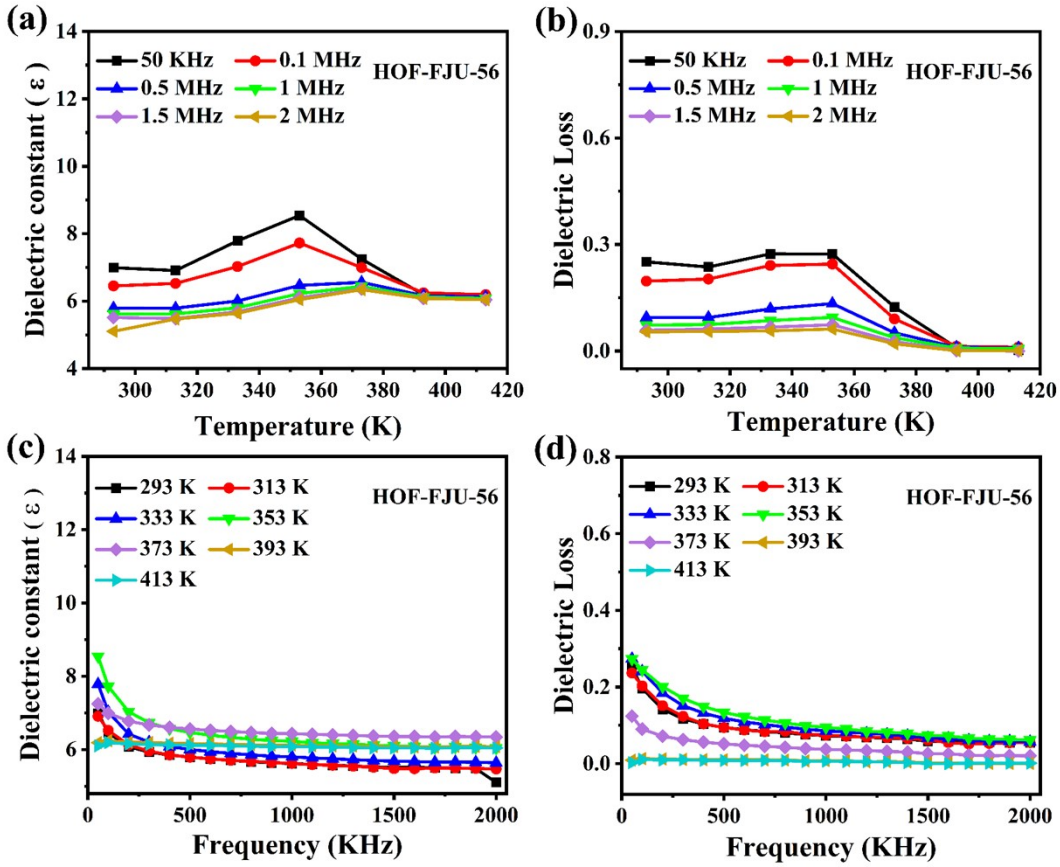


**Fig. S3** Temperature-dependent dielectric constant (a) and dielectric loss (b) of **HOF-FJU-56** at different frequencies; Frequency-dependent dielectric constant (c) and dielectric loss (d) of **HOF-FJU-56** at different temperatures.

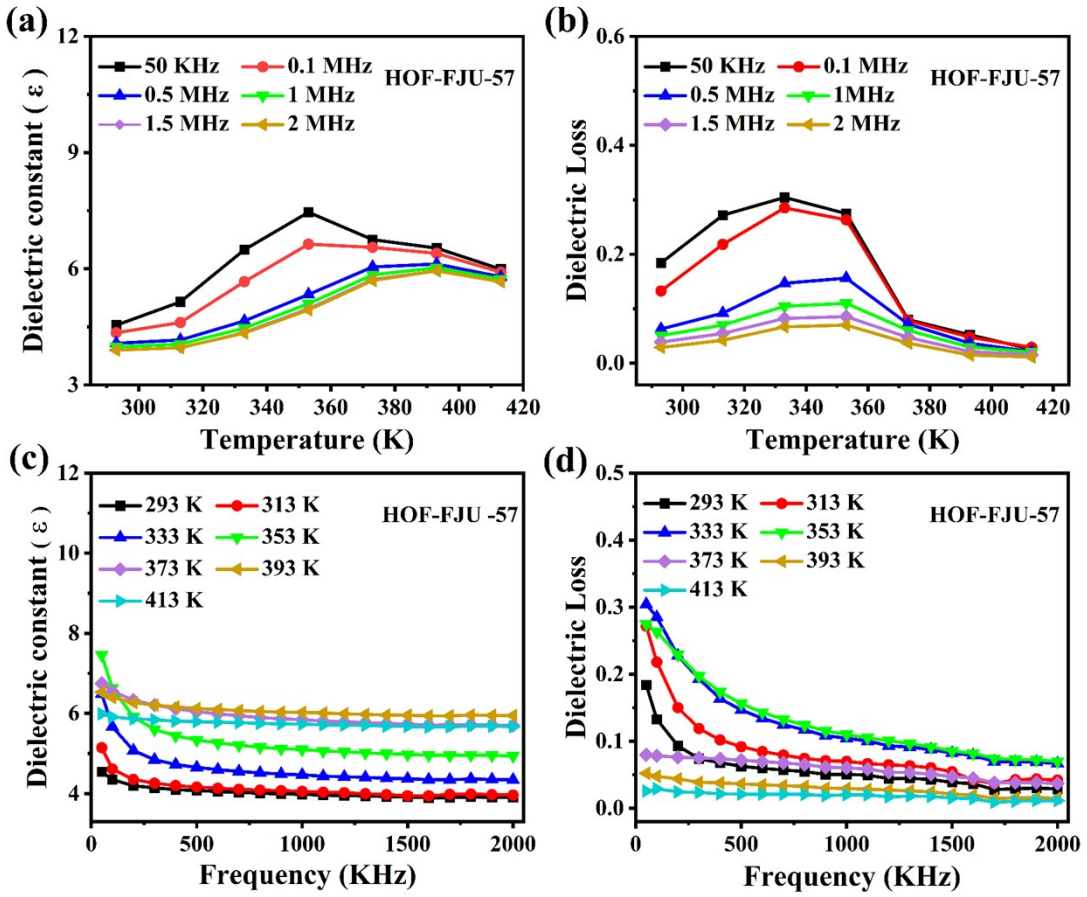


**Fig. S4** Temperature-dependent dielectric constant (a) and dielectric loss (b) of **HOF-FJU-57** at different frequencies; Frequency-dependent dielectric constant (c) and dielectric loss (d) of **HOF-FJU-57** at different temperatures.

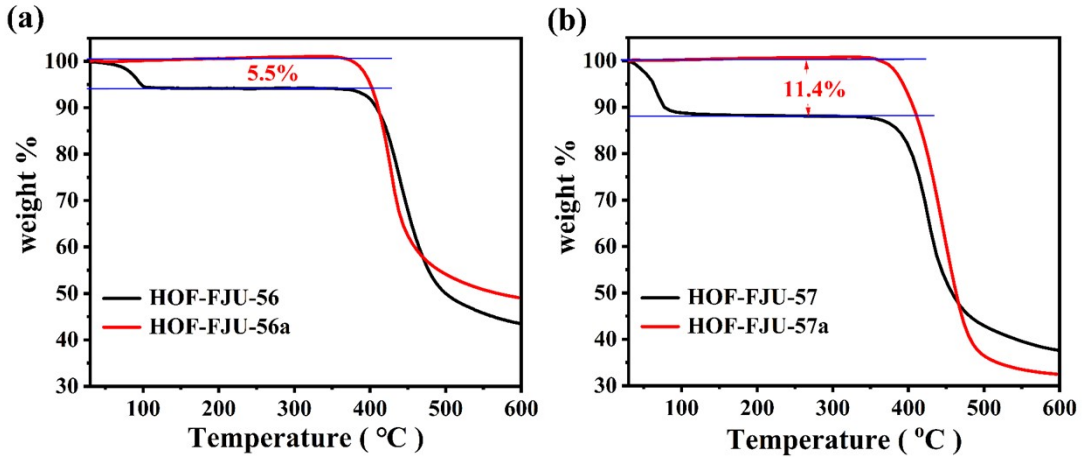


**Fig. S5** Thermogravimetric plots for (a) **HOF-FJU-56, HOF-FJU-56a** and (b) **HOF-FJU-57, HOF-FJU-57a**.

To determine the thermal properties of these two crystals, thermogravimetric analysis (TGA) is performed from 30°C to 600°C under $N_2$ atmosphere. As shown in Fig. S5, the first weight loss rates of **HOF-FJU-56** and **HOF-FJU-57** are approximately 5.5% and 11.4%, respectively, which are consistent with the theoretically calculated solvent loss rates of 5.16% and 11.6% from their crystal data. The second weight loss of the two materials occurred at around 370 °C, which may be due to the decomposition of TQBTC.

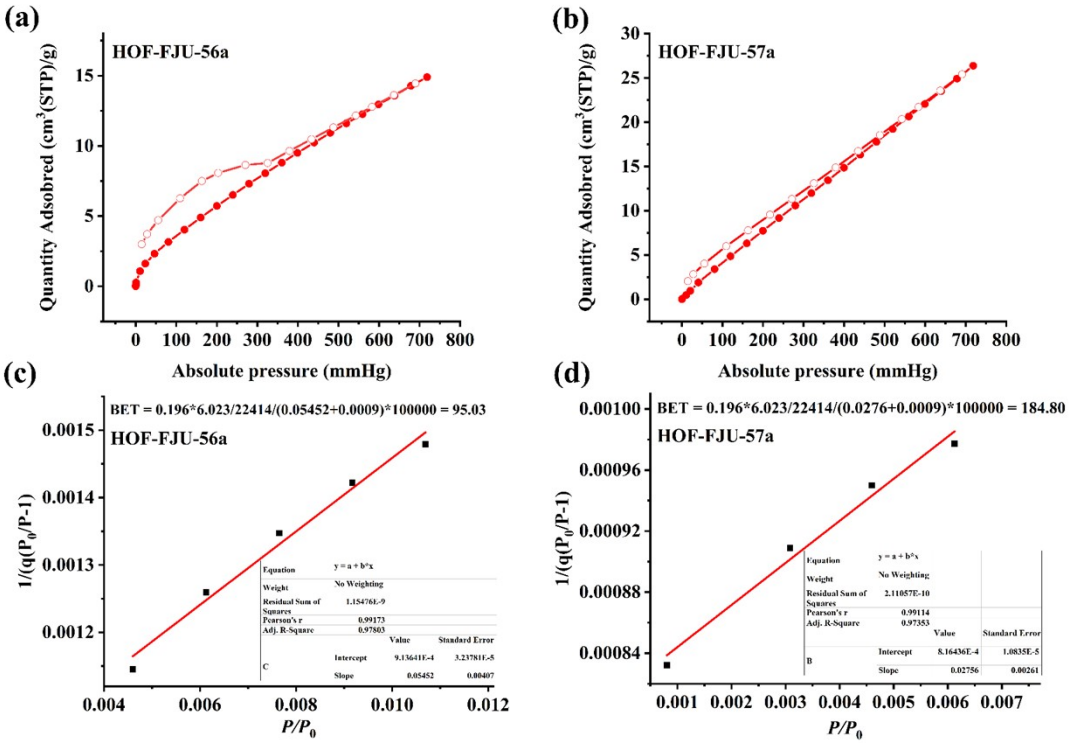


**Fig. S6** $CO_2$ sorption isotherm at 196 K of **HOF-FJU-56a** (a) and **HOF-FJU-57a** (b). The BET plots for **HOF-FJU-56a** (c) and **HOF-FJU-57a** (d).

$S_{BET}$ = 0.196*6.023/22414/(slope+intercept)*100000

$S_{BET(HOF\text{-}FJU\text{-}56a)}$ = 0.196*6.023/22414/(0.05452+0.0009)*100000=95.03 $m^2/g$

$S_{BET(HOF\text{-}FJU\text{-}57a)}$ = 0.196*6.023/22414/(0.02760+0.0009)*100000=184.80 $m^2/g$

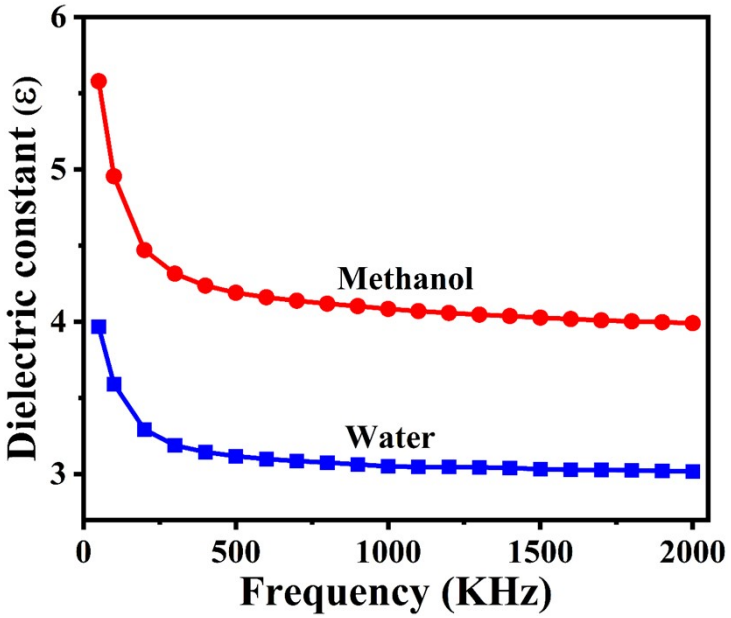


**Fig. S7** Frequency-dependent dielectric constants of **HOF-FJU-57a** after immersion in methanol and water, respectively, at 298k.

**Table S1** Crystallographic Data for **HOF-FJU-56** and **HOF-FJU-57**.

| | **HOF-FJU-56** | **HOF-FJU-57** |
|---|---|---|
| CCDC | 2241066 | 2245969 |
| Empirical formula | $C_{37}H_{27}N_6O_4$ | $C_{37}H_{33}N_6O_{6.5}$ |
| Formula weight | 619.64 | 665.69 |
| Temperature/K | 150.00(10) | 149.99(10) |
| Crystal system | triclinic | triclinic |
| Space group | *P1* | *P-1* |
| a/Å | 4.8338(5) | 8.9567(6) |
| b/Å | 12.1052(8) | 12.2826(7) |
| c/Å | 13.0176(11) | 15.4474(6) |
| $\alpha$/° | 101.200(7) | 72.697(4) |
| $\beta$/° | 90.866(7) | 86.055(4) |
| $\gamma$/° | 97.392(7) | 88.054(5) |
| Volume/Å$^3$ | 740.37(11) | 1618.48(16) |
| Z | 1 | 2 |
| $\rho_{calc}$g/cm$^3$ | 1.39 | 1.366 |
| $\mu$/mm$^{-1}$ | 0.756 | 0.786 |
| F(000) | 323.0 | 698.0 |
| Radiation | Cu Kα ($\lambda$ = 1.54184) | Cu Kα ($\lambda$ = 1.54184) |
| Data/restraints/parameters | 4306/3/426 | 6143/6/459 |
| Goodness-of-fit on $F^2$ | 1.085 | 1.005 |
| Final R indexes [I>=2σ (I)] | $R_1$ = 0.0695, $wR_2$ = 0.1776 | $R_1$ = 0.0887, $wR_2$ = 0.2266 |
| Final R indexes [all data][a] | $R_1$ = 0.0823, $wR_2$ = 0.1919 | $R_1$ = 0.1346, $wR_2$ = 0.2532 |

[a]$R_1 = \sum(|F_o| - |F_c|) / \sum|F_o|$ , [b]$wR_2 = [\sum w(F_o^2 - F_c^2)^2 / \sum w(F_o^2)^2]^{0.5}$

**Table S2.** Compare the dielectric constant and dielectric loss of different materials at 1MHz, 298K.

| Compound | Leakage current at 0.5 KV/cm | Dielectric constant | dielectric loss | The range of test temperature | Ref. |
|---|---|---|---|---|---|
| **HOF-FJU-56a** | **$1.06\times10^{-10}$** | **4.06** | **0.009** | **13-413 K** | **This work** |
| **HOF-FJU-57a** | **$1.45\times10^{-13}$** | **2.12** | **0.067** | **13-413 K** | **This work** |
| $[Zn(CEIC)_2(H_2O)]\cdot2DMF$ | / | 3.90 | 0.067 | 303-363K | 1 |
| TAPB-$TPOC_6$-COF film | $1.4\times10^{-10}$ | 1.25 | 0.010 | 293-433K | 2 |
| FMOF-1 | / | 1.28 | / | 298K | 3 |
| TmBPHF | / | 2.09 | 0.001 | 298-573K | 4 |
| $[Zn_2(Hbbim)_2(bbim)]n$ | / | 3.05 | 0.019 | 3.5-350K | 5 |
| TmBPPA | / | 2.23 | 0.009 | 293-573K | 6 |
| SiCOH | $1.0\times10^{-10}$ | 3.48 | 0.009 | 298-523K | 7 |
| GD50 | $2\times10^{-10}$ | 3.16 | / | 298K | 8 |
| HGD50 | $7\times10^{-11}$ | 3.03 | / | 298K | 8 |
| Silica film | $1.0\times10^{-8}$ | 2.0 | 0.020 | 298K | 9 |
| PSZ MFI low-κ film | $1.35\times10^{-8}$ | 1.83 | / | 298K | 10 |
| MSQ film | $6.0\times10^{-12}$ | 2.7 | / | 298K | 11 |
| BC:H | $6.0\times10^{-13}$ | 3.3 | / | 298K | 12 |
| ZIF-8 film | $3.0\times10^{-12}$ | 2.3 | 0.008 | 298-473K | 13 |
| ZIF-67 film | / | 2.39 | 0.060 | 298K-423K | 14 |

**References**


1. S. -S. Yu, G. -J. Yuan, and H. -B. Duan, The low dielectric constant and relaxation dielectric behavior in hydrogen-bonding metal–organic frameworks. *RSC. Adv.*, 2015, **5**, 45213-45216.
2. P. Shao, J. Li, F. Chen, L. Ma, Q. Li, M. Zhang, J. Zhou, A. Yin, X. Feng, and B. Wang, Flexible Films of Covalent Organic Frameworks with Ultralow Dielectric Constants under High Humidity. *Angew. Chem. Int. Ed. Engl.*, 2018, **57**, 16501-16505.
3. S. Galli, A. Cimino, J. F. Ivy, C. Giacobbe, R. K. Arvapally, R. Vismara, S. Checchia, M. A. Rawshdeh, C. T. Cardenas, W. K. aseen, A. Maspero, and M. A. Omary, Fluorous Metal–Organic Frameworks and Nonporous Coordination Polymers as Low-$\kappa$ Dielectrics. *Adv. Funct. Mater.*, 2019, **29**, 1904707.
4. C. Qian, R. Bei, T. Zhu, W. Zheng, S. Liu, Z. Chi, M. P. Aldred, X. Chen, Y. Zhang, J. Xu, Facile Strategy for Intrinsic Low-$\kappa$ Dielectric Polymers: Molecular Design Based on Secondary Relaxation Behavior. *Macromolecules.*, 2019, **52**, 4601-4609.
5. S. Mendiratta, M. Usman, C. C. Chang, Y. C. Lee, J. W. Chen, M. K. Wu, Y. C. Lin, C. P. Hsu, and K. L. Lu, Zn(II)-based metal-organic framework: an exceptionally thermally stable, guest-free low dielectric material. *J. Mater. Chem. C.*, 2017, **5**, 1508-1513.
6. C. Qian, Z.-G. Fan, E. -W. Zheng, R. -X. Bei, T. -W. Zhu, S. -W. Liu, Z. -G. Chi, M. -P. Aldred, X. -D. Chen, Y. Zhang, and J. -R. Xu, A Facile Strategy for Non-fluorinated Intrinsic Low-$\kappa$ and Low-loss Dielectric Polymers: Valid Exploitation of Secondary Relaxation Behaviors. Chinese. *J. Polym. Sci.*, 2019, **38**, 213-219.
7. S. Kwak, R. Jeong, and S. Rhee, Nanocomposite Low-$\kappa$ SiCOH Films by Direct PECVD Using Vinyltrimethylsilane. *J. Electrochem. Soc.*, 2004, **151**, 0013-4651.
8. S. Yang, S. Y. Kwak, J. Jin, and B. S. Bae, Highly condensed epoxy-oligosiloxane-based hybrid material for transparent low-$\kappa$ dielectric coatings. *ACS Appl. Mater. Interfaces.*,2009, **1**, 1585-90.
9. S. Yu, T. Wong, and K. Pita, Surface modified silica mesoporous films as a low dielectric constant intermetal dielectric. *J. Appl. Phys.*, 2002, **92**, 3338-3344.

10. H. Lu, C. Teng, C. Yu, Y. Liu, and B. Wan, Addition of Surfactant Tween 80 in Coating Solutions for Making Mesoporous Pure Silica Zeolite MFI Low-$\kappa$ Films. *Ind. Eng. Chem. Res.*, 2010, **49**, 6279–6286.
11. T. Chang, P. Liu, Y. Mor, S. Sze, Y. Yang, M. Feng, F. Pan, B. Dai, and C. Chang, The Novel Improvement of Low Dielectric Constant Methylsilsesquioxane by $N_2O$ Plasma Treatment. *J. Electrochem. Soc.*, 1999, **146**, 3802-3806.
12. B. J. Nordell, T. D. Nguyen, C. L. Keck; S. Dhungana, A. N. Caruso, W. A. Lanford, J. T. Gaskins, P. E. Hopkins, D. R. Merrill, D. C. Johnson, L. L. Ross, P. Henry, S. W. King, and M. M. Paquette, Conquering the Low-$\kappa$ Death Curve: Insulating Boron Carbide Dielectrics with Superior Mechanical Properties. *Adv. Electron. Mater.*, 2016, **2**, 1600073.
13. S. Eslava, L. Zhang, S. Esconjauregui, J. Yang, K. Vanstreels, M. R. Baklanov, E. Saiz, Metal-OrganicFramework ZIF-8 Films as Low-$\kappa$ Dielectrics in Microelectronics. *Chem. Mater.*, 2012, **25**, 27-33.
14. M. Krishtab, I. Stassen, T. Stassin, A. J. Cruz, O. O. Okudur, S. Armini, C. Wilson, S. Gendt, Lu, K. L, and R. Ameloot, Vapor-deposited zeolitic imidazolate frameworks as gap-filling ultra-low-κ dielectrics. *Nat. Commun.*, 2019, **10**, 3729.